IEEE Access
Multidisciplinary ⋮ Rapid Review ⋮ Open Access Journal

Received 13 February 2023, accepted 12 March 2023, date of publication 28 March 2023, date of current version 4 April 2023.

Digital Object Identifier 10.1109/ACCESS.2023.3262554

RESEARCH ARTICLE

The Prediction of Badminton Flight Trajectory Based on an Intelligent Compensator

CHIH-HUI CHIU[1], JUNG-LLI SU[2], AND CHIEH-MIN LIN[1]
[1]Department of Communications, Navigation and Control Engineering, National Taiwan Ocean University, Jhongjheng, Keelung 20224, Taiwan
[2]Office of Physical Education, Chung-Yuan Christian University, Chung-Li 32023, Taiwan

Corresponding author: Chih-Hui Chiu (chchiu@ntou.edu.tw)

ABSTRACT A real-time visual servo badminton trajectory tracking system (VSBTTS) is proposed in this study. VSBTTS is composed of two parts: the image unit and the tracking operation unit. The primary function of the image unit is to segment the moving shuttlecock from a continuous image taken by the camera and detect the moving object. The tracking operation unit is used to track parts of the shuttlecock found in the image unit. Then, the flight trajectory of the shuttlecock is estimated; however, it is difficult for tracking operation units to avoid estimation errors, preventing them from achieving full accuracy. In this study, a fuzzy compensation controller is used to compensate for the system estimation errors of the flight trajectory. Using the fuzzy compensator, the trajectory of the shuttlecock is accurately estimated. Experimental results demonstrate the usefulness of the proposed shuttlecock trajectory tracking system.

INDEX TERMS Badminton trajectory tracking system, real-time visual servo system, fuzzy compensator.

I. INTRODUCTION

With the development of image scientific technologies, many image technological applications that have not be implemented due to computational complexities are now practical. In particular, computer vision technology has been developed, which makes the application of computer vision increasingly important. The application of visual servo systems has thus become extensive; for example, a visual servo system can be used is semiconductor and optoelectronic industries, optical fiber alignment systems, and auxiliary mechanical arms for grabbing objects. In defense and military applications, a visual servo system can be used for face recognition to prevent terrorists from entering a given country, or image recognition can be used to mark the location of enemy military facilities in satellite photos. Increasing activities of criminal organizations also markedly increase the demand for security monitoring. Visual servo systems can also be used in daily life, such as traffic monitoring, home security, crime detection and personnel identification [1], [2], [3], [4], [5].

The associate editor coordinating the review of this manuscript and approving it for publication was Wenbing Zhao.

Many coaches and athletes know that motion analysis is a useful training tool. With the aid of motion analysis, athletes can watch their own performance repeatedly, which can help them to better understand their strengths and weaknesses. However, a real-time video tracking system is rarely used in the athlete training process as a basis for testing the effectiveness of self-practice. Although there are many offline video programs available that can help players understand their shortcomings, such offline aids are not as effective as instant systems.

Over the past decade, vision-based systems such as Hawk-Eye have provided ball tracking for enhanced broadcast visualizations and aiding umpiring decisions in both tennis and cricket. Hawk-Eye is the most popular vision-based system, and the Hawk-Eye tennis ball tracking system was presented in [6]. This system is used in the sports broadcasting field. To date, the Hawk-Eye system has been the most representative technology [7], [8] and is famous for delivering the most reliable and innovative advertising solutions in sports. The Hawk-Eye system has led to the development of a number of additional services that are changing the face of sports production. Hawk-Eye's vision processing, video replay and creative graphical technologies make sports fairer and more engaging. These vision-based technologies are flexible and

can be adapted to create products that suit the unique requirements of each sport with which people work.

However, badminton is a special case because the shuttlecock is not sphere-shaped and weighs only approximately 5 grams. Its flight process is affected by rotation, feather damage, and wind direction. A vision-based system calculates landing points by capturing flight trajectories; thus, the difficulty in calculating shuttlecock landing points is much higher than that of other balls. The timing of a stroke is the key element for making contact with the shuttlecock and affects the hitting quality. Therefore, an effective shuttlecock flight tracking system is proposed in this study. Most past studies considered the speed of shuttlecocks, and few studies have investigated flight trajectory compensation of a shuttlecock.

In [9], the primary goal was to construct and validate a motion equation for the flight of the badminton and to find the relationship between the air resistance force and a shuttlecock's speed. That method was based on the motion laws of aerodynamics and applied aerodynamic theories to construct the motion equation of a shuttlecock's flying trajectory under the effects of gravitational force and air resistance force. In [10], a visual trajectory estimation method using blur characteristics in the 3D space was proposed. The authors acquired a speed vector based on the shape of a motion blur region. That method can extract both the position and speed of the moving object from an image frame, and apply them to a visual tracking process using a Kalman filter. In [11], a method to estimate the position of a small moving object was proposed. The authors reported that it is difficult to fit a dynamic model of a target object moving fast and anomalously, and thus focused on a phenomenon in which a high-velocity moving object is observed as a line-shaped region in captured images by motion blur. In [12], the proposed method could be used by coaches and players to assess and improve short serve accuracy. The authors reported that this method is more representative of a match environment because the shuttlecock rarely lands due to the opponent returning the serve. In [13], the authors studied the flip phenomenon and the dynamics of the flight, and then discussed implications on the game; a possible classification of different shots was also proposed. In [14], they also showed that their trajectory is completely different from a classical parabola. In the end, the effect of aerodynamic drag on shuttlecock dynamics was proposed.

This study discusses how to detect the movement and displacement of the shuttlecock using continuous images taken by a camera based on a microprocessor. Then, the flight trajectory of the shuttlecock is determined using a 2D coordinate image plane. A fuzzy compensation controller is used to compensate for the error between the theoretical value and the real value of the shuttlecock flight trajectory.

Compared with traditional approaches, a fuzzy controller (FC) is designed based on human experience. An FC can be designed without system information. Recently, fuzzy logic technology has been applied to many applications. In [15], an omnidirectional inverted pendulum is controlled based on a Takagi-Sugeno (TS) fuzzy algorithm. The authors reported that the omnidirectional inverted pendulum was a custom system that used two TS fuzzy control approaches for omnidirectional inverted pendulum system control. An embedded control center is the core of the omnidirectional inverted pendulum. A disturbance observer-based adaptive fuzzy finite-time control issue for strict-feedback nonlinear systems was studied in [16]. For practical application requirements, that method can guarantee that the system error moves into the prescribed bounded set in a known time. To improve the effect of the Exp-Sign activation function and the Sinh-Sign activation function on the convergence and robustness of the zeroing neural network model. In [17], two fuzzy adaptive activation functions were constructed using a Mamdani fuzzy logic controller. In [18], a single-wheel system was designed and implemented. Such a single-wheel vehicle is a custom system that consists of a platform, a wheel, and a DC motor with a gearbox. A Mamdani fuzzy controller is used for this single-wheel system real-time control.

In this study, a real-time visual servo badminton tracking experimental system is proposed. The real-time visual servo badminton tracking system is composed of two parts: the image processing unit and the trajectory operation unit. The primary function of the image processing unit is to segment the moving shuttlecock from the continuous image taken by the camera. In this study, background subtraction [19] is used to detect moving objects because the number of required computations is less than that of other moving object detection methods. The primary function of the trajectory operation unit is to take the flight trajectory of the shuttlecock found in the image unit into the dynamic equation of a free projectile to estimate the complete flight trajectory of the shuttlecock. However, it is difficult for dynamic equations to achieve truly accurate trajectories without estimation errors. In this study, fuzzy theory is used to analyze the uncertain dynamic model; to estimate the speed and hitting point of badminton; and to accurately judge the timing of batting. Then, in the future, a badminton player can determine the best hitting time with the aid of the proposed badminton tracking system. Moreover, this research may have a more long-term application value such as military and semiconductor industries.

II. INTELLIGENT TRACKING SYSTEM

A. IDEAL FREE PROJECTILE

Assuming that air resistance is not accounted for, the schematic diagram of a well-known free projectile is shown in Fig. 1.

In a two-dimensional coordinate system, the quadratic equation of a parabolic trajectory is as follows:

$$y = az^2 + bz + c \tag{1}$$

where y is the pixel value of the vertical axis coordinate; z is the pixel value of the horizontal axis coordinate; and a, b, and c are the parameters of the parabolic equation. Assuming that any three points in this parabolic trajectory are (z_1, y_1), (z_2, y_2), and (z_3, y_3), substituting these three points

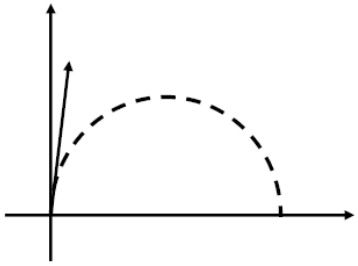

FIGURE 1. Schematic diagram of free projectile.

into Eq. (1) can be used to form the matrix shown below:

$$\begin{bmatrix} y_1 \\ y_2 \\ y_3 \end{bmatrix} = \begin{bmatrix} z_1^2 & z_1 & 1 \\ z_2^2 & z_2 & 1 \\ z_3^2 & z_3 & 1 \end{bmatrix} \cdot \begin{bmatrix} a \\ b \\ c \end{bmatrix} \tag{2}$$

Using a mathematical method to obtain a, b, and c, the two-dimensional quadratic equation of a parabolic trajectory can be obtained. Then, the flying quadratic equation can be well defined. When the shuttlecock can be viewed by the camera, the ideal badminton parabolic trajectory parameters can be calculated based on the real-time image of any continuous three shuttlecock real pixels, (z_1, y_1), (z_2, y_2), and (z_3, y_3).

However, air resistance is always unknown in practical applications. Therefore, the ideal shuttlecock trajectory should not be precisely obtained. In this study, an intelligent tracking system (ITS) is proposed to compensate for the predicted trajectory error caused by air resistance when the shuttlecock is flying. In this study, a fuzzy compensation controller is used to compensate for the badminton flight trajectory error. The fuzzy compensation controller system block diagram is shown in Fig. 2.

B. FUZZY COMPENSATION CONTROLLER

First, the pixel coordinates (z, y) of the shuttlecock are captured by the camera module. For simplification, the height plays a key role in predicting the real trajectory in this study. Combining the height from Eq. (2) and the real height obtained by the camera module, the intelligent tracking system can provide a compensation value to modify the ideal value.

The following description is a review of a fuzzy system mechanism. In general, a fuzzy system mechanism is a collection of fuzzy rules. A fuzzy rule $Rule^j, j = 1, \ldots, m$, where m is the number of fuzzy rules, is presented in the following form:

$$Rule^j : \text{If } x_1 \text{ is } \mu_{A_1}^j, \ldots, x_n \text{ is } \mu_{A_n}^j, \text{ then } u_j \text{ is } \mu_{B_j} \tag{3}$$

where $u_j, j = 1, \ldots, m$ is the output variable; x_i, $i = 1, \ldots, n$ are the input variables; n is the number of inputs; $\mu_{A_1}, \ldots, \mu_{A_n}$ are standard fuzzy sets; and $\mu_{B_1}, \ldots, \mu_{B_m}$ are fuzzy singletons.

The defuzzification method of the fuzzy mechanism is the center-of-gravity defuzzification method with the product- sum operation in this study. Thus, the fuzzy system mechanism u can be described by:

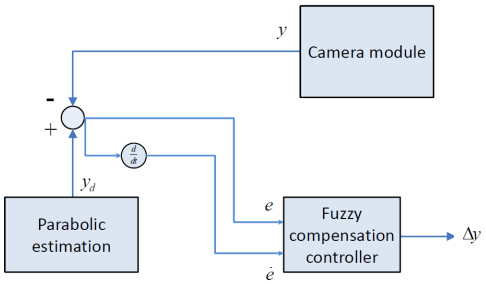

FIGURE 2. Tracking system architecture diagram.

$$u = \frac{\sum_{j=1}^{m} v_j \prod_{i=1}^{n} \mu_{A_i}^j(x_i)}{\sum_{j=1}^{m} \prod_{i=1}^{n} \mu_{A_i}^j(x_i)} \tag{4}$$

where v_j is the point where $\mu_{B_j} = 1$. The tracking error, e, and the error variation, $\dot{e}$, are the inputs of the proposed intelligent fuzzy tracking system shown in Eqs. (5) and (6):

$$e(N) = y_d(N) - y(N) \tag{5}$$

$$\dot{e}(N) = e(N) - e(N-1) \tag{6}$$

where y_d is the height from Eq. (1) and N is the discrete time.

The inputs of the fuzzy system are the trajectory error (e) and the error variation ($\dot{e}$). The input variables are transformed into the fuzzy quantity of fuzzy inference using the membership functions. In this fuzzy compensator, the triangle function is used as the fuzzy input membership function, and the output membership function is in the form of a singleton value.

Theorem1: We consider the aforementioned fuzzy system, where (a) the output of the fuzzy system equals zero when $e(t) \cdot \dot{e}(t) \leq 0$; (b) the output of the fuzzy system is less than $-e(t)$ when $e(t)$ is larger than zero and $e(t) \cdot \dot{e}(t) > 0$; or (c) the output of the fuzzy system is larger than $-e(t)$ when $e(t)$ is less than zero and $e(t) \cdot \dot{e}(t) > 0$. Thus, the system error convergence of the fuzzy system can be guaranteed.

Proof: First, the Lyapunov function candidate is chosen as $V(e(t), \dot{e}(t)) = (e^2(t) + \dot{e}^2(t))/2$. Then:

$$\dot{V} = e(t)\dot{e}(t) + \dot{e}(t)\ddot{e}(t). \tag{7}$$

Because the error acceleration of the system is proportional to the system input, according to Newton's second law, $\ddot{e} = ku$, where k is a positive constant. For $\dot{V} \leq 0$, $e(t)$ and $\dot{e}(t)$ must have opposite signs and $\ddot{e}(t) = 0$ when $e(t) \cdot \dot{e}(t)$ is larger than zero and $\ddot{e}(t) = ku < -e(t)$ when $e(t)$ is larger than zero or when $e(t) \cdot \dot{e}(t)$ is larger than zero and $\ddot{e}(t) = ku > -e(t)$ when $e(t)$ is less than zero. Then:

$$\dot{V} = e(t)\dot{e}(t) + \dot{e}(t)\ddot{e}(t) \leq 0. \tag{8}$$

Because $\dot{V}(t) \leq 0$, $\dot{V}(t)$ is negative and semidefinite (i.e., $\dot{V}(t) \leq \dot{V}(0)$), which implies that $e(t)$ and $\dot{e}(t)$ are bounded. Because $V(e(0), \dot{e}(0))$ is bounded and $V(t)$ is nonincreasing

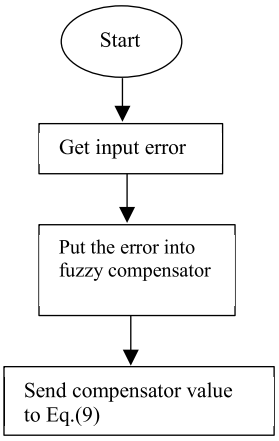

FIGURE 3. Program flow chart.

and bounded, by Barbalat's Lemma [20], it can imply that $e(t)$ and $\dot{e}(t)$ converge to zero as $t \to \infty$.

In this study, the defuzzification method of the fuzzy mechanism is a center of gravity defuzzification method with the minimum inference engine. Finally, the fuzzy system output (u) can be obtained. Then, the next prediction height value, y_P, is described by the following equation:

$$y_P(N+1) = y_d(N) + u \tag{9}$$

Fig. 3 shows the program flow chart. Algorithm 1 is the 86duino One to calculate the fuzzy compensator value.

Algorithm 1 Fuzzy Controller Algorithm

Input: system error $\boldsymbol{E}$, system error variation $\boldsymbol{DE}$, mean value of membership function. **Output:** compensator value u

1. Limit the input variable into the interval between the largest mean value and the smallest mean value
   If $E <$ smallest mean value, $E =$ smallest mean value;
   if $E >$ largest mean value, $E =$ largest mean value;
   if $DE <$ smallest mean value, $DE =$ smallest mean value;
   if $DE >$ largest mean value, $DE =$ largest mean value;
2. Calculate the fuzzy membership function
3. Calculate the output of the fuzzy control algorithm by the center of gravity defuzzification as:

$u = (\mathrm{u11} + \mathrm{u12} + \mathrm{u21} + \mathrm{u22})/(\mathrm{w11} + \mathrm{w12} + \mathrm{w21} + \mathrm{w22})$

End Algorithm

III. EXPERIMENTAL RESULTS

In this section, a real-world experimental system is described, and then, an experimental procedure is proposed. Finally, the experimental results are shown and discussed.

The inputs of the fuzzy system are the trajectory error (e) and the error variation ($\dot{e}$). The input variables are transformed into the fuzzy quantity of fuzzy inference using the membership functions. In this fuzzy compensator, the Gaussian function is used as the fuzzy input membership function. In this study, the Gaussian function is represented as:

$$A(x) = \exp\left(\frac{-(x-\lambda)^2}{\sigma^2}\right) \tag{10}$$

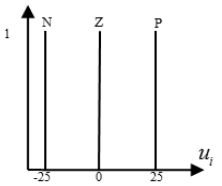

FIGURE 4. Output membership functions of the fuzzy compensator.

TABLE 1. Fuzzy rules base.

e / $\dot{e}$	N	Z	P
N	P	Z	Z
Z	Z	Z	Z
P	Z	Z	N

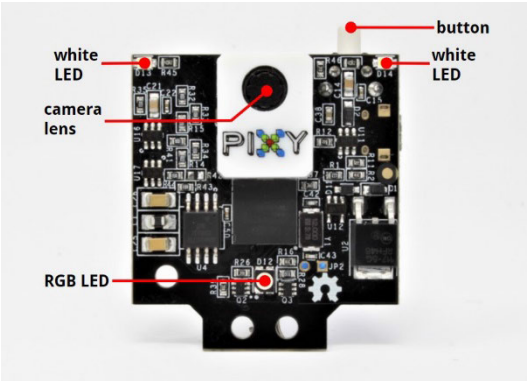

FIGURE 5. CMUcam5 Pixy2 vision sensor [21].

FIGURE 6. Schematic diagram of the experiment.

where $A(x)$ is the fuzzy input membership function with the mean λ and the variance σ. In this study, the means of the trajectory error (e) are -7, 0, and 4.5; and the means of the error variation ($\dot{e}$) are -15, 0, and 16.5. The variance of the trajectory error and the variance of the error variation are 1 and 400, respectively. The output membership function of the fuzzy compensator takes the form of a singleton value. Fig. 4 is the output membership function of the fuzzy compensator. Negative (N), zero (ZO), and positive (P) are used as the fuzzy variables in this fuzzy compensator. Table 1 is the fuzzy rule base for the fuzzy compensator.

The camera module used in this study is a CMUcam5 Pixy2 open source vision sensor, as shown in Fig. 5. CMUcam5 has many advantages, including being lightweight and

TABLE 2. CMUcam5 Pixy2 specifications.

processor	NXP LPC4330, 204 MHz, dual core
Image sensor	Aptina MT9M114, 1296×976 resolution
Perspective	75 degrees horizontal, 47 degrees vertical
Lens field-of-view	60 degrees horizontal, 40 degrees vertical
Input Current	140 mA typical
Input voltage	USB input (5 V) or unregulated input (6 V to 10 V)
Random access memory (RAM)	264 Kbyte
Flash	2 Mbytes
Available data output pipeline	UART serial, SPI, I2C, USB, digital, analog
volume	1.5" x 1.65" x 0.6"
weight	10 grams
Sampling rate	60 frames per second

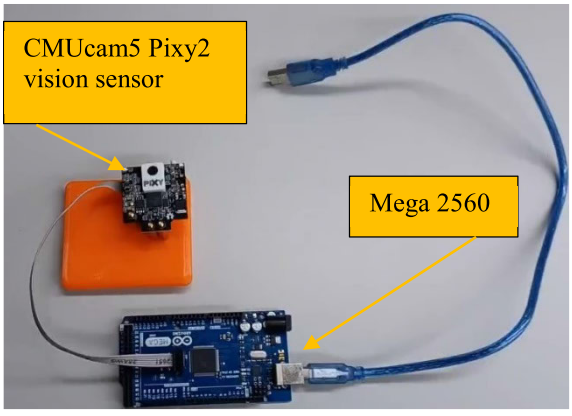

FIGURE 7. Full view of the experimental system.

thin; having high precision and low power consumption; etc. This sensor has a built-in microprocessor that can perform image recognition and uses background subtraction and connected component algorithms to identify objects of a specific color. In this study, CMUcam5 is used with an Arduino Mega 2560 controller.

The specifications of the CMUcam5 Pixy2 vision sensor are shown in Table 2 [21].

TABLE 3. Arduino® Mega 2560 Rev3 technical specifications.

Microcontroller	ATmega2560	
USB connector	USB-B	
Pins	Built-in LED Pin	13
	Digital I/O Pins	54
	Analog input pins	16
	PWM pins	15
Communication	UART	Yes, 4
	I2C	Yes
	SPI	Yes
Power	I/O Voltage	5 V
	Input voltage (nominal)	7-12 V
	DC Current per I/O Pin	20 mA
	Supported battery	9 V battery
	Power Supply Connector	Barrel Plug
Clock speed	Main Processor	ATmega2560 16 MHz
	USB-Serial Processor	ATmega16U2 16 MHz
Memory	ATmega2560	8KB SRAM, 256KB FLASH, 4KB EEPROM
Dimensions	Weight	37 g
	Width	53.3 mm
	Length	101.5 mm

According to the CMUcam5 Pixy2 Specifications, the processor speed of the CMUcam5 Pixy2 is 204 MHZ. The sampling rate of the CMUcam5 Pixy2 is 60 frames per second. The energy consumption of the CMUcam5 Pixy2 is approximately 700 mW.

Fig. 6 shows the experimental process diagram. Then, the flight trajectory of the shuttlecock is determined using a 2D coordinate image plane and is reported as a real-world image captured by the camera module (CMUcam5 Pixy vision sensor). Fig. 6(a) to Fig. 6(e) are in order as the shuttlecock moves from right to left on the camera. First, the shuttlecock is thrown into the sky, as shown in Fig. 6(a). Then, the shuttlecock follows a parabolic trajectory. Fig. 7 shows the experimental system in this study.

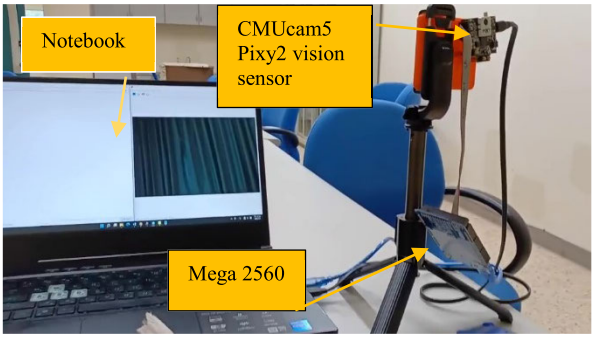

FIGURE 8. Full view of the experimental hardware system.

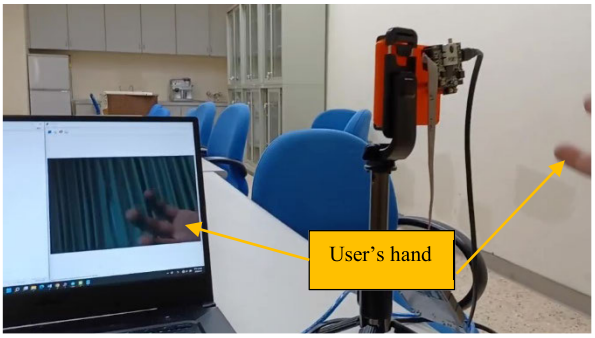

FIGURE 9. CMUcam5 Pixy2 test diagram.

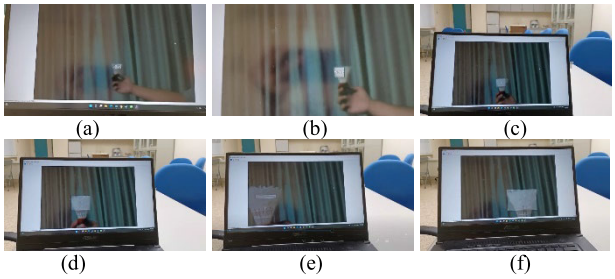

FIGURE 10. Shuttlecock captured by the CMUcam5 Pixy2 test diagrams.

The embedded controller used in this study is the Arduino Mega 2560 controller, which is a high-performance board based on an 8-bit microcontroller. The Mega 2560 has 54 digital I/O pins, of which 15 pins can generate pulse-width modulation (PWM); 16 analog input pins; 4096 bytes of EEPROM, which is not erased when powered off; 4× hardware serial ports (UARTs); and a clock speed of 16 MHz. The proposed control algorithm was coded in the Mega 2560 integrated development environment (IDE), and the syntax of the Mega 2560 IDE is similar to C/C++ and Arduino IDE syntax. The technical specifications for the Arduino® Mega 2560 Rev3 are shown in Table 3 [22].

According to the Arduino Mega 2560 technical specifications, the clock speed of the primary processor is 16 MHz. the chip has an upper limit of 200 mA for all processing and IO combined, and 200 mA is the maximum current between VCC and GND. Therefore, the energy consumption of the Arduino Mega 2560 is no more than 1 W.

Next, the experimental procedure will be described in detail. Fig. 8 shows the total experimental hardware system

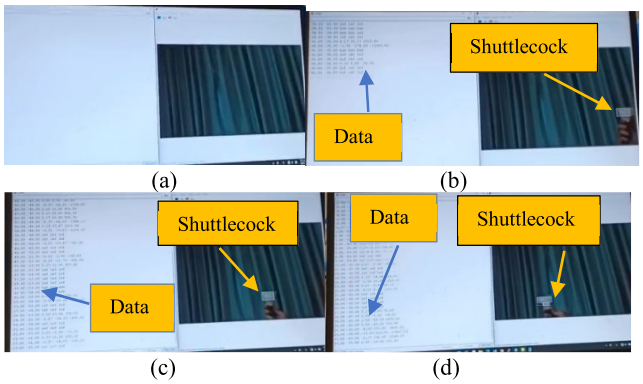

FIGURE 11. Schematic diagram of the shuttlecock real image and data.

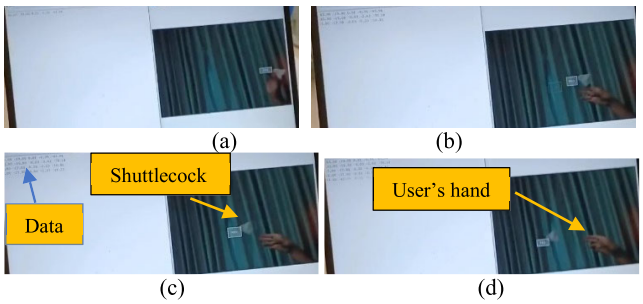

FIGURE 12. Schematic diagram of the shuttlecock free flight real image and data.

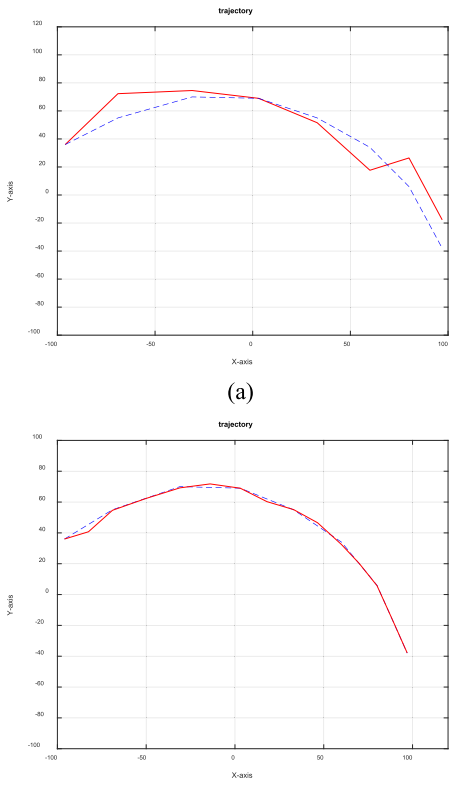

FIGURE 13. First test dataset: (a) Experimental results without the fuzzy compensator. (b) Experimental results with the fuzzy compensator.

combined with the CMUcam5 Pixy2 vision sensor, the Mega 2560, and a laptop in this study. The CMUcam5 Pixy2 vision

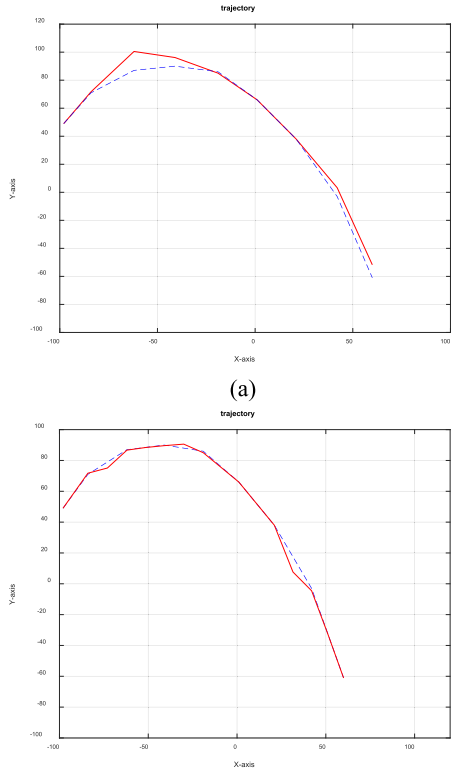

FIGURE 14. Second test dataset: (a) Experimental results without the fuzzy compensator. (b) Experimental results with the fuzzy compensator.

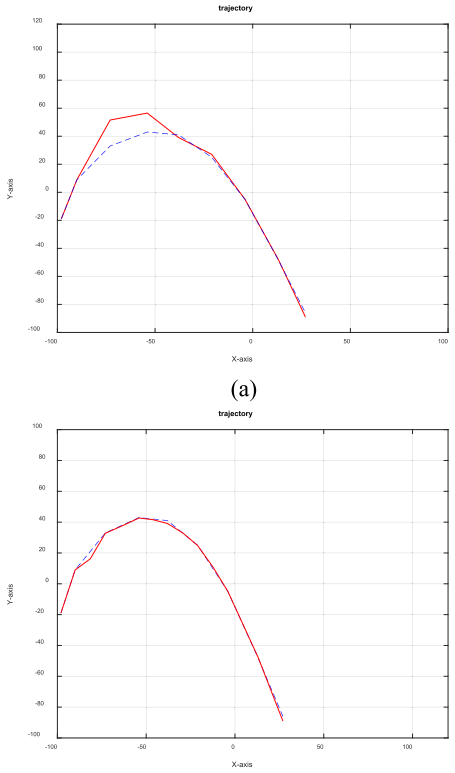

FIGURE 15. Third test dataset: (a) Experimental results without the fuzzy compensator. (b) Experimental results with the fuzzy compensator.

sensor is used to identify the location of the shuttlecock. Mega 2560 is used to drive the CMUcam5 Pixy2 vision sensor and transfer the real shuttlecock trajectory data to the laptop, which displays the shuttlecock's real image and receives the real shuttlecock trajectory data.

Fig. 9 is the CMUcam5 Pixy2 test diagram. The user's hand is placed in front of the CMUcam5 Pixy2. Then, the hand image is also shown in the notebook monitor.

Fig. 10 shows the shuttlecock captured by the CMUcam5 Pixy2 test diagram. The shuttlecock is held by a user's hand. Fig. 11(a) to Fig. 11(f) are the shuttlecock random moving in the air. In this study, CMUcam5 Pixy2 is set to capture white objects. Images of the shuttlecock are captured by the Pixy2, as shown in Fig. 10.

Fig. 11 is the CMUcam5 Pixy2 experimental test process diagram. The shuttlecock is held by a user's hand during the test. Fig. 11(a) to Fig. 11(d) are in accordance with the order of the shuttlecock from right to left on the camera. Fig. 11(a) is the original monitor image. In Fig. 11(b) to Fig. 11(d), the shuttlecock trajectory data are shown on the left-hand side of the notebook monitor. The right-hand side of the notebook monitor is the shuttlecock image.

Fig. 12 is the shuttlecock free flight real-world image captured by the CMUcam5 Pixy2 vision sensor. In Fig. 12, the user throws the shuttlecock in front of the camera. Fig. 12(a) to Fig. 12(d) are in order as the shuttlecock moves from right to left across the camera.

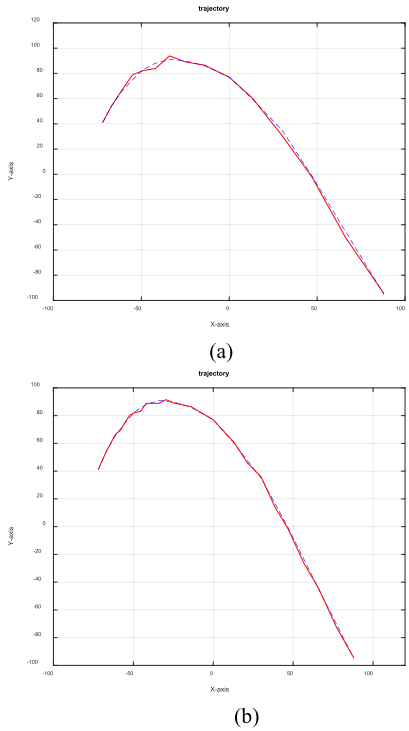

FIGURE 16. Fourth test dataset: (a) Experimental results without the fuzzy compensator. (b) Experimental results with the fuzzy compensator.

According to the above description, the real shuttlecock trajectory data are captured by the CMUcam5 Pixy2

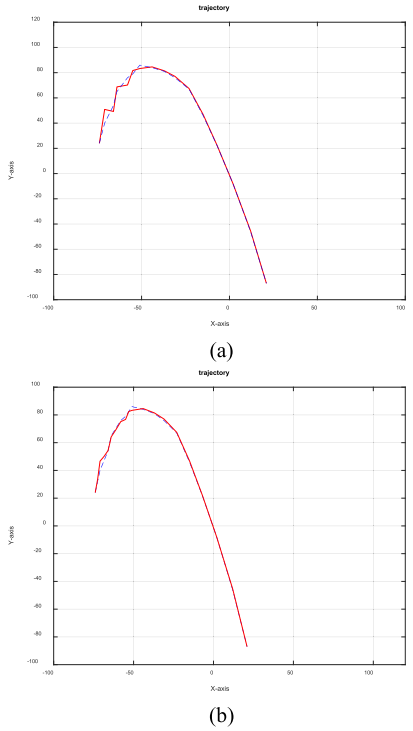

FIGURE 17. Fifth test dataset: (a) Experimental results without the fuzzy compensator. (b) Experimental results with the fuzzy compensator.

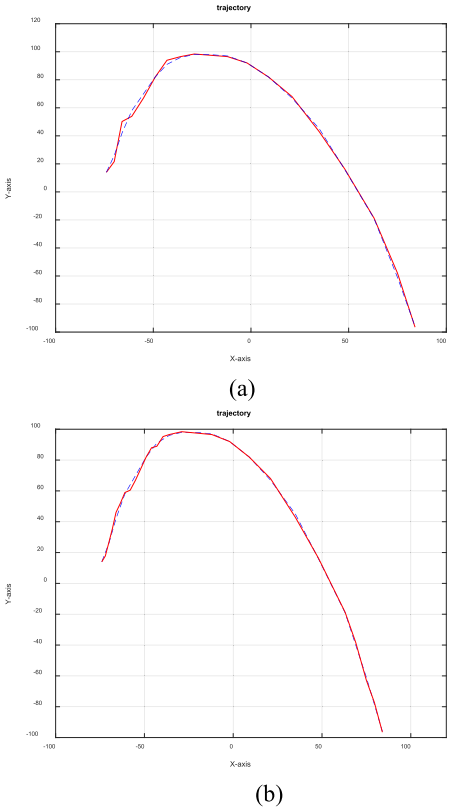

FIGURE 18. Sixth test dataset: (a) Experimental results without the fuzzy compensator. (b) Experimental results with the fuzzy compensator.

vision sensor. Then, the shuttlecock trajectory is drawn using MATLAB. In this study, several piecewise parabola

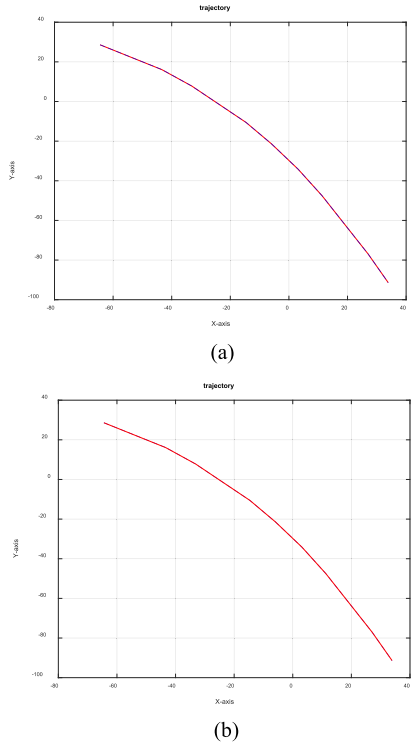

FIGURE 19. A badminton drop shot is hit by a racket (I): (a) Experimental results without the fuzzy compensator. (b) Experimental results with the fuzzy compensator.

TABLE 4. System performance indicators.

	Without fuzzy compensator	With fuzzy compensator
First test data	143.1458	2.5776
Second test data	33.6193	7.2703
Third test data	54.4255	2.3410
Fourth test data	4.2507	1.5330
Fifth test data	8.1292	2.5775
Sixth test data	4.7745	2.1496

trajectories in every experimental test are described. For example, based on Eq. (1), a parabola trajectory can be drawn when $(z_1, y_1), (z_2, y_2), and (z_3, y_3)$ are obtained. $(z_2, y_2), (z_3, y_3), and (z_4, y_4)$ can also draw another new parabola trajectory. The interpolation method is used in this study. Based on the interpolation method, more shuttlecock pixels can be used for trajectory estimation of the shuttlecock.

In this study, six test datasets are presented. Fig. 13(a) and Fig. 13(b) show comparison results for the first test data between the method without and with the fuzzy compensator. In Fig. 13(a), the dotted line is the real shuttlecock trajectory, and the solid line is the parabolic trajectory based on Eq. 1. The two lines have completely different trajectories. In Fig. 13(b), the two trajectories are exactly aligned; the powerful effect of the proposed parabolic trajectory prediction method

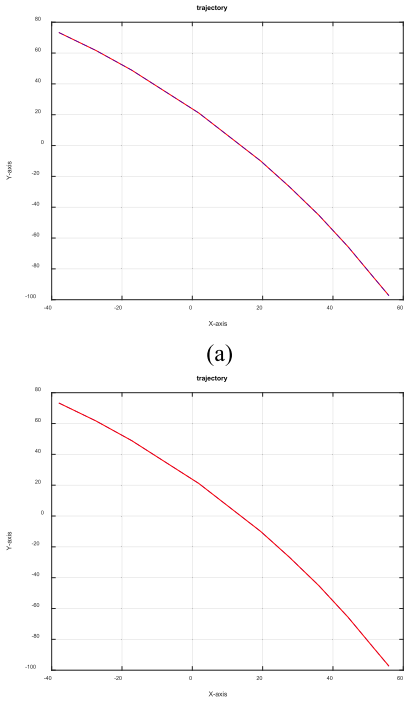

FIGURE 20. A badminton drop shot is hit by a racket (II): (a) Experimental results without the fuzzy compensator. (b) Experimental results with the fuzzy compensator.

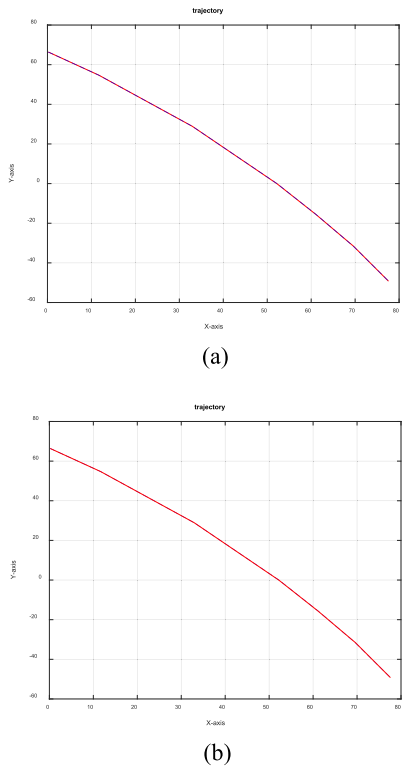

FIGURE 21. A badminton drop shot is hit by a racket (III): (a) Experimental results without the fuzzy compensator. (b) Experimental results with the fuzzy compensator.

is verified. There are 8 shuttlecock real pixels in Fig. 13. Fig. 14 and Fig. 15 show comparison results for the second

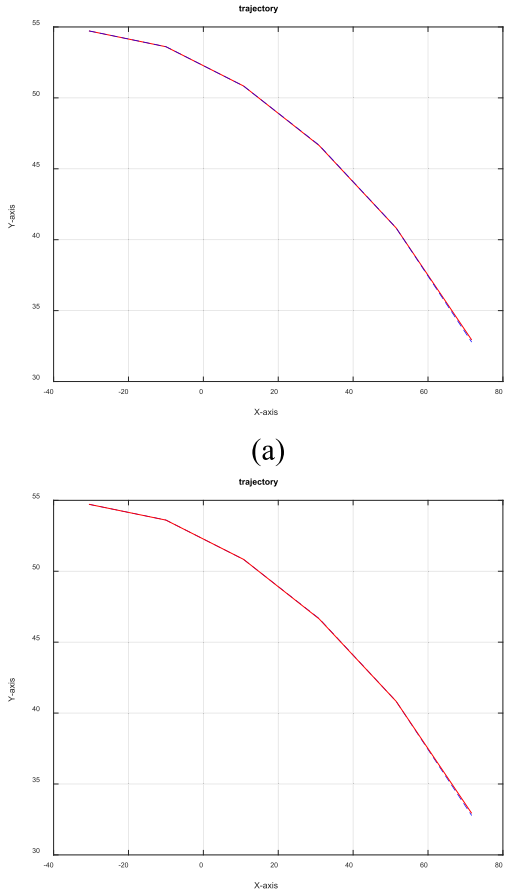

FIGURE 22. A badminton drop shot is hit by a racket (IV): (a) Experimental results without the fuzzy compensator. (b) Experimental results with the fuzzy compensator.

test data and the third test data, respectively. There are 9 pixels in Fig. 14 and Fig. 15. The parabolic trajectory prediction method with a fuzzy compensator is always more accurate than the method without a fuzzy compensator. Fig. 16, Fig. 17, and Fig. 18 are the fourth test data, the fifth test data, and the sixth test data, respectively. There are 15 shuttlecock image pixels, 16 image pixels, and 19 image pixels in Fig. 16, Fig. 17, and Fig. 18, respectively. The parabolic trajectory prediction method with a fuzzy compensator is always better than the method without a fuzzy compensator.

To quantify the performance of the system, the mean square error (MSE) is used as a system performance indicator [23]. MSE is defined by Eq. (6) below:

$$MSE = \frac{1}{N}\sum_{i=1}^{N} e^2(i), \tag{11}$$

where N is the number of data samples.

The performance indicators of the above six test datasets are shown in Table 3.

Table 3 shows that the performance indicators (MSEs) of the six test data have marked differences with or without

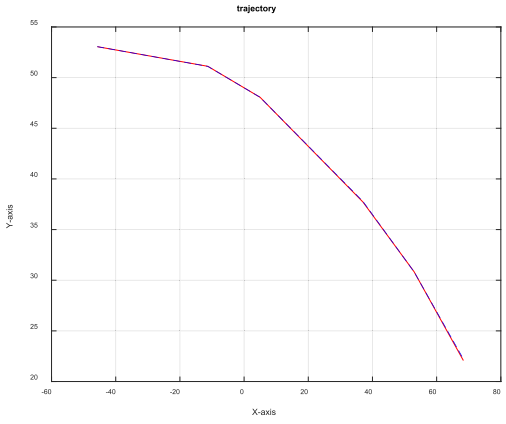

(a)

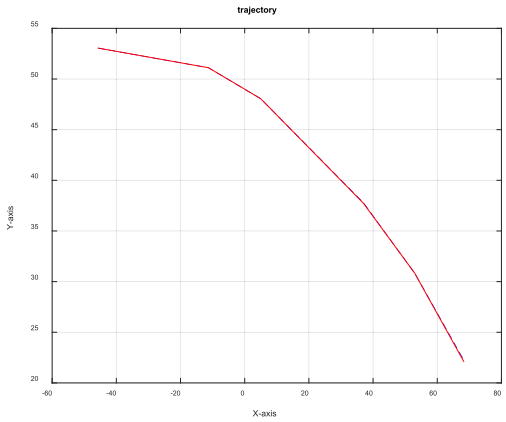

(b)

FIGURE 23. A badminton drop shot is hit by a racket (V): (a) Experimental results without the fuzzy compensator. (b) Experimental results with the fuzzy compensator.

the fuzzy compensator. The fuzzy compensator is shown to improve prediction accuracy.

For the real system test, a new camera module (an Intel RealSense D415) is used at a sampling rate of approximately 90 frames per second. A badminton drop shot is hit by a racket, and Figs. 19-23 show the experimental results.

The Intel RealSense D415 can capture the badminton's position when it is hit by a racket. The shuttlecock speed when hit by a racket is higher than the shuttlecock speed when thrown by the player's hand. According to the above experimental results, the prediction badminton trajectories based on Eq. 1 are sufficiently close to the real trajectories because the shuttlecock trajectory hit by a racket is similar to a straight line. However, the fuzzy compensator can still improve prediction accuracy.

For a more comprehensive example, one more example is provided when disturbances are added. Based on Fig. 19, Fig. 24(a) shows the result when the parabolic trajectory based on Eq. 1 is not correct. However, in Fig. 24(b), the two trajectories are nearly exactly matched in Fig. 19(b). Clearly, the powerful effect of the proposed fuzzy compensator prediction method is ensured even if the speed of the shuttlecock is higher than other examples.

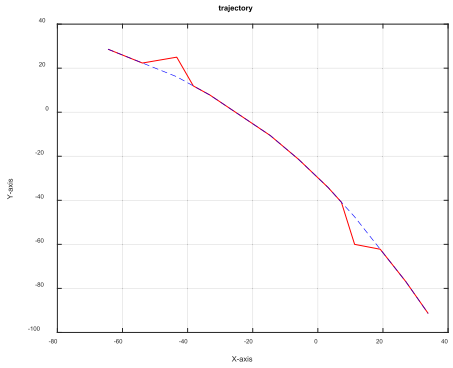

(a)

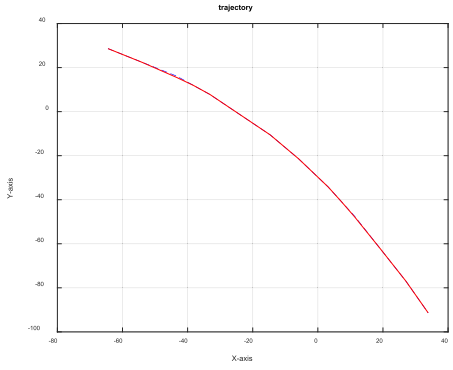

(b)

FIGURE 24. A badminton drop shot is hit by a racket, and disturbances are added: (a) Experimental results without the fuzzy compensator. (b) Experimental results with the fuzzy compensator.

IV. CONCLUSION

In this study, by combining a fuzzy compensator with an ideal dynamic equation of a free projectile, the real flight trajectory of a shuttlecock is estimated. This proposed system makes the prediction of the flying trajectory of a shuttlecock nearly perfectly accurate. The flight trajectory predicted by the parabolic equation is modified based on a fuzzy compensator to improve the accuracy of the calculated shuttlecock trajectory. Concurrently, with the proposed system, flight trajectory prediction of the moving shuttlecock can be performed in the real world. The performance indicators (MSEs) show the difference with or without a fuzzy compensator. The fuzzy compensator is useful for shuttlecock trajectory real-world prediction. In the future, this system should be used as a tool to perform moving object trajectory detection in the sky. This system can also be used in badminton robot implementation. Based on the proposed system, the estimated trajectory of the shuttlecock flight path is the same as the real trajectory. Therefore, the hitting area after the highest point of the shuttlecock flight path is confirmed. Then, a hitting area can be suggested for the badminton robot to accurately hit the shuttlecock. In my future works, neural network-based machine learning techniques will be used. Neural network-based machine learning techniques are more nonlinearly robust than fuzzy theory and will have better tracking performance in terms of error compensation.

REFERENCES

[1] Z. He, C. Wu, S. Zhang, and X. Zhao, "Moment-based 2.5-D visual servoing for textureless planar part grasping," *IEEE Trans. Ind. Electron.*, vol. 66, no. 10, pp. 7821–7830, Oct. 2019.

[2] D. Zheng, H. Wang, J. Wang, S. Chen, W. Chen, and X. Liang, "Image-based visual servoing of a quadrotor using virtual camera approach," *IEEE/ASME Trans. Mechatronics*, vol. 22, no. 2, pp. 972–982, Apr. 2017.

[3] X. Zhang, Y. Fang, X. Zhang, J. Jiang, and X. Chen, "A novel geometric hierarchical approach for dynamic visual servoing of quadrotors," *IEEE Trans. Ind. Electron.*, vol. 67, no. 5, pp. 3840–3849, May 2020.

[4] F. Xu, H. Wang, Z. Liu, and W. Chen, "Adaptive visual servoing for an underwater soft robot considering refraction effects," *IEEE Trans. Ind. Electron.*, vol. 67, no. 12, pp. 10575–10586, Dec. 2020.

[5] M. A. Rafique and A. F. Lynch, "Output-feedback image-based visual servoing for multirotor unmanned aerial vehicle line following," *IEEE Trans. Aerosp. Electron. Syst.*, vol. 56, no. 4, pp. 3182–3196, Aug. 2020.

[6] N. Owens, "Hawk-eye tennis system," in *Proc. Int. Conf. Vis. Inf. Eng.*, 2003, pp. 182–185.

[7] X. Wei, P. Lucey, S. Morgan, and S. Sridharan, "Forecasting the next shot location in tennis using fine-grained spatiotemporal tracking data," *IEEE Trans. Knowl. Data Eng.*, vol. 28, no. 11, pp. 2988–2997, Nov. 2016.

[8] C. Zhang, F. Yang, G. Li, Q. Zhai, Y. Jiang, and D. Xuan, "MV-sports: A motion and vision sensor integration-based sports analysis system," in *Proc. IEEE INFOCOM Conf. Comput. Commun.*, Apr. 2018, pp. 1070–1078.

[9] L.-M. Chen, Y.-H. Pan, and Y.-J. Chen, "A study of shuttlecock's trajectory in badminton," *J. Sports Sci. Med.*, vol. 8, pp. 657–662, Dec. 2009.

[10] H. Shishido, I. Kitahara, Y. Kameda, and Y. Ohta, "A trajectory estimation method for badminton shuttlecock utilizing motion blur," in *Proc. 6th Pacific Rim Symp. Image Video Technol. (PSIVT)*, 2013, pp. 325–336.

[11] H. Shishido, Y. KamedaI, I. Kitahara, and Y. Ohta, "Trajectory estimation of a fast and anomalously moving badminton shuttle," in *Proc. Int. Workshop Adv. Image Technol.*, 2015, pp. 11–13.

[12] S. Vial, J. Cochrane, A. J. Blazevich, and J. L. Croft, "Using the trajectory of the shuttlecock as a measure of performance accuracy in the badminton short serve," *Int. J. Sports Sci. Coaching*, vol. 14, no. 1, pp. 91–96, Feb. 2019.

[13] C. Cohen, B. D. Texier, D. Quéré, and C. Clanet, "The physics of badminton," *New J. Phys.*, vol. 17, no. 6, Jun. 2015, Art. no. 063001.

[14] B. D. Texier, C. Cohen, D. Quéré, and C. Claneta, "Shuttlecock dynamics," *Proc. Eng.*, vol. 34, pp. 176–181, Jan. 2012.

[15] C.-H. Chiu, Y.-T. Hung, and Y.-F. Peng, "Design of a decoupling fuzzy control scheme for omnidirectional inverted pendulum real-world control," *IEEE Access*, vol. 9, pp. 26083–26092, 2021.

[16] J. Qiu, T. Wang, K. Sun, I. J. Rudas, and H. Gao, "Disturbance observer-based adaptive fuzzy control for strict-feedback nonlinear systems with finite-time prescribed performance," *IEEE Trans. Fuzzy Syst.*, vol. 30, no. 4, pp. 1175–1184, Apr. 2022.

[17] J. Dai, X. Yang, L. Xiao, L. Jia, and Y. Li, "ZNN with fuzzy adaptive activation functions and its application to time-varying linear matrix equation," *IEEE Trans. Ind. Informat.*, vol. 18, no. 4, pp. 2560–2570, Apr. 2022.

[18] C.-H. Chiu, "Adaptive fuzzy control strategy for a single-wheel transportation vehicle," *IEEE ACCESS*, vol. 7, pp. 113272–113283, 2019.

[19] W. Brand, "Morphable 3D models from video," in *Proc. IEEE Comput. Soc. Conf. Comput. Vis. Pattern Recognit.*, Dec. 2001, pp. 456–463.

[20] C.-H. Chiu and C.-C. Chang, "Wheeled human transportation vehicle implementation using output recurrent fuzzy control strategy," *IET Control Theory Appl.*, vol. 8, no. 17, pp. 1886–1895, 2014.

[21] *Wiki—CMUcam5 Pixy—CMUcam—Open Source Programmable Embedded Color Vision Sen-Sors*. [Online]. Available: https://docs.pixycam.com/wiki/doku.php?id=wiki:v2:overview

[22] *Technical Specifications for the Arduino Mega 2560 Rev3*. [Online]. Available: https://docs.arduino.cc/hardware/mega-2560

[23] C. H. Chiu and W. R. Tsai, "Design and implementation of an omnidirectional spherical mobile platform," *IEEE Trans. Ind. Electron.*, vol. 62, no. 3, pp. 1619–1628, Mar. 2015.

CHIH-HUI CHIU was born in Taiwan. He received the B.S. degree in electrical engineering from the Tatung Institute of Technology, Taipei, Taiwan, in 1994, and the M.S. and Ph.D. degrees in electrical engineering from National Central University, Taiwan, in 1996 and 2000, respectively.

He is currently a Professor with the Department of Communications, Navigation and Control Engineering, National Taiwan Ocean University, Keelung, Taiwan. His research interests include fuzzy logic theory, intelligent control, robots, mechatronics, and control theory applications.

JUNG-LLI SU was born in Taiwan. He received the M.S. degree from National Taiwan Sport University, Taoyuan, Taiwan, in 1996. Since 1996, he has been with the Office of Physical Education, Chung-Yuan Christian University, Chung-Li, Taiwan, where he is currently a Professor. His research interests include fuzzy neural networks and badminton.

CHIEH-MIN LIN was born in Taiwan. He received the B.S. and M.S. degrees in electrical engineering from Yuan-Ze University, Taoyuan, Taiwan. His research interests include fuzzy logic theory, intelligent control, and control theory applications.